
Incorporating Interpretable Output Constraints in Bayesian Neural Networks

Wanqian Yang
Harvard University
Cambridge, MA, USA
yangw@college.harvard.edu

Lars Lorch*
ETH Zürich
8092 Zürich, Switzerland
llorch@student.ethz.ch

Moritz A. Graule
Harvard University
Cambridge, MA, USA
graulem@g.harvard.edu

Himabindu Lakkaraju
Harvard University
Cambridge, MA, USA
hlakkaraju@seas.harvard.edu

Finale Doshi-Velez
Harvard University
Cambridge, MA, USA
finale@seas.harvard.edu

Abstract

Domains where supervised models are deployed often come with task-specific constraints, such as prior expert knowledge on the ground-truth function, or desiderata like safety and fairness. We introduce a novel probabilistic framework for reasoning with such constraints and formulate a prior that enables us to effectively incorporate them into Bayesian neural networks (BNNs), including a variant that can be amortized over tasks. The resulting Output-Constrained BNN (OC-BNN) is fully consistent with the Bayesian framework for uncertainty quantification and is amenable to black-box inference. Unlike typical BNN inference in uninterpretable parameter space, OC-BNNs widen the range of functional knowledge that can be incorporated, especially for model users without expertise in machine learning. We demonstrate the efficacy of OC-BNNs on real-world datasets, spanning multiple domains such as healthcare, criminal justice, and credit scoring.

1 Introduction

In domains where predictive errors are prohibitively costly, we desire models that can both capture predictive uncertainty (to inform downstream decision-making) as well as enforce prior human expertise or knowledge (to induce appropriate model biases). Performing Bayesian inference on deep neural networks, which are universal approximators [11] with substantial model capacity, results in BNNs — models that combine high representation power with quantifiable uncertainty estimates [21, 20]¹. The ability to encode informative functional beliefs in BNN priors can significantly reduce the bias and uncertainty of the posterior predictive, especially in regions of input space sparsely covered by training data [27]. Unfortunately, the trade-off for their versatility is that BNN priors, defined in high-dimensional parameter space, are uninterpretable. A general approach for incorporating functional knowledge (that human experts might possess) is therefore intractable.

Recent work has addressed the challenge of incorporating richer functional knowledge into BNNs, such as preventing miscalibrated model predictions out-of-distribution [9], enforcing smoothness constraints [2] or specifying priors induced by covariance structures in the dataset (cf. Gaussian processes) [25, 19]. In this paper², we take a different direction by tackling functional knowledge expressed as *output constraints* — the set of values y is constrained to hold for any given x . Unlike other types of functional beliefs, output constraints are intuitive, interpretable and easily specified,

*Work done while at Harvard University.

¹See Appendix A for a technical overview of BNN inference and acronyms used throughout this paper.

²Our code is publicly available at: <https://github.com/dtak/ocbnn-public>.

even by domain experts without technical understanding of machine learning methods. Examples include ground-truth human expertise (e.g. known input-output relationship, expressed as scientific formulae or clinical rules) or critical desiderata that the model should enforce (e.g. output should be restricted to the permissible set of safe or fair actions for any given input scenario).

We propose a sampling-based prior that assigns probability mass to BNN parameters based on how well the BNN output obeys constraints on drawn samples. The resulting **Output-Constrained BNN** (OC-BNN) allows the user to specify any constraint directly in its functional form, and is amenable to all black-box BNN inference algorithms since the prior is ultimately evaluated in parameter space.

Our contributions are: **(a)** we present a formal framework that lays out what it means to learn from output constraints in the probabilistic setting that BNNs operate in, **(b)** we formulate a prior that enforces output constraint satisfaction on the resulting posterior predictive, including a variant that can be amortized across multiple tasks, **(c)** we demonstrate proof-of-concepts on toy simulations and apply OC-BNNs to three real-world, high-dimensional datasets: (i) enforcing physiologically feasible interventions on a clinical action prediction task, (ii) enforcing a racial fairness constraint on a recidivism prediction task where the training data is biased, and (iii) enforcing recourse on a credit scoring task where a subpopulation is poorly represented by data.

2 Related Work

Noise Contrastive Priors Hafner et al. [9] propose a generative “data prior” in function space, modeled as zero-mean Gaussians if the input is out-of-distribution. Noise contrastive priors are similar to OC-BNNs as both methods involve placing a prior on function space but performing inference in parameter space. However, OC-BNNs model output constraints, which encode a richer class of functional beliefs than the simpler Gaussian assumptions encoded by NCPs.

Global functional properties Previous work have enforced various functional properties such as Lipschitz smoothness [2] or monotonicity [29]. The constraints that they consider are different from output constraints, which can be defined for local regions in the input space. Furthermore, these works focus on classical NNs rather than BNNs.

Tractable approximations of stochastic process inference Garnelo et al. [7] introduce neural processes (NP), where NNs are trained on sequences of input-output tuples $\{(\mathbf{x}, y)_i\}_{i=1}^m$ to learn distributions over functions. Louizos et al. [19] introduce a NP variant that models the correlation structure of inputs as dependency graphs. Sun et al. [25] define the BNN variational objective directly over stochastic processes. Compared to OC-BNNs, these models represent a distinct direction of work, since (i) VI is carried out directly over function-space terms, and (ii) the set of prior functional assumptions is different; they cannot encode output constraints of the form that OC-BNNs consider.

Equality/Inequality constraints for deep probabilistic models Closest to our work is that of Lorenzi and Filippone [18], which incorporates equality and inequality constraints, specified as differential equations, into regression tasks. Similar to OC-BNNs, constraint (\mathcal{C}) satisfaction is modeled as the conditional $p(Y, \mathcal{C}|\mathbf{x})$, e.g. Gaussian or logistic. However, we (i) consider a broader framework for reasoning with constraints, allowing for diverse constraint formulations and defined for both regression *and classification* tasks, and (ii) verify the tractability and accuracy of our approach on a comprehensive suite of experiments, in particular, high-dimensional tasks.

3 Notation

Let $\mathbf{X} \in \mathcal{X}$ where $\mathcal{X} = \mathbb{R}^Q$ be the input variable and $Y \in \mathcal{Y}$ be the output variable. For regression tasks, $\mathcal{Y} = \mathbb{R}$. For K -classification tasks, \mathcal{Y} is any set with a bijection to $\{0, 1, \dots, K - 1\}$. We denote the ground-truth mapping (if it exists) as $f^* : \mathcal{X} \rightarrow \mathcal{Y}$. While f^* is unknown, we have access to observed data $D_{tr} = \{\mathbf{x}_i, y_i\}_{i=1}^N$, which may be noisy or biased. A conventional BNN is denoted as $\Phi_{\mathbf{W}} : \mathcal{X} \rightarrow \mathcal{Y}$. $\mathbf{W} \in \mathcal{W}$, where $\mathcal{W} = \mathbb{R}^M$, are the BNN parameters (weights and biases of all layers) represented as a flattened vector. All BNNs that we consider are multilayer perceptrons with RBF activations. Uppercase notation denotes random variables; lowercase notation denotes instances.

4 Output-Constrained Priors

In joint $\mathcal{X} \times \mathcal{Y}$ space, our goal is to constrain the output y for any set of inputs \mathbf{x} . In this setting, classical notions of “equality” and “inequality” (in constrained optimization) respectively become *positive* constraints and *negative* constraints, specifying what values y can or cannot take.

Definition 4.1. A *deterministic output constraint* \mathcal{C} is a tuple $(\mathcal{C}_x, \mathcal{C}_y, \circ)$ where $\mathcal{C}_x \subseteq \mathcal{X}$, $\mathcal{C}_y : \mathcal{C}_x \rightarrow 2^{\mathcal{Y}}$ and $\circ \in \{\in, \notin\}$. \mathcal{C} is *satisfied* by an output y iff $\forall \mathbf{x} \in \mathcal{C}_x, y \circ \mathcal{C}_y(\mathbf{x})$. $\mathcal{C}^+ := \mathcal{C}$ is a *positive constraint* if \circ is \in . $\mathcal{C}^- := \mathcal{C}$ is a *negative constraint* if \circ is \notin . \mathcal{C} is a *global constraint* if $\mathcal{C}_x = \mathcal{X}$. \mathcal{C} is a *local constraint* if $\mathcal{C}_x \subset \mathcal{X}$.

The distinction between positive and negative constraints is not trivial because the user typically has access to only one of the two forms. Positive constraints also tend to be more informative than negative constraints. Definition 4.1 alone is not sufficient as we must define what it means for a BNN, which learns a predictive *distribution*, to satisfy a constraint \mathcal{C} . A natural approach is to evaluate the probability mass of the prior predictive that satisfies a constraint.

Definition 4.2. A *deterministic output constraint* $\mathcal{C} = (\mathcal{C}_x, \mathcal{C}_y, \circ)$ is ϵ -*satisfied* by a BNN with prior $\mathbf{W} \sim p(\mathbf{w})$ if, $\forall \mathbf{x} \in \mathcal{C}_x$ and for some $\epsilon \in [0, 1]$:

$$\int_{\mathcal{Y}} \mathbb{I}[y \circ \mathcal{C}_y(\mathbf{x})] \cdot p(\Phi_{\mathbf{W}} = y | \mathbf{x}) dy \geq 1 - \epsilon \quad (1)$$

where $p(\Phi_{\mathbf{W}} | \mathbf{x}) := \int_{\mathcal{W}} p(\Phi_{\mathbf{w}}(\mathbf{x}) | \mathbf{x}, \mathbf{w}) p(\mathbf{w}) d\mathbf{w}$ is the BNN prior predictive.

The strictness parameter ϵ can be related to *hard* and *soft* constraints in optimization literature; the constraint is hard iff $\epsilon = 0$. Note that ϵ is not a parameter of our prior, instead, (1) is the goal of inference and can be empirically evaluated on a test set. Since BNNs are probabilistic, we can generalize Definition 4.1 further and specify a constraint directly as some distribution over \mathcal{Y} :

Definition 4.3. A *probabilistic output constraint* \mathcal{C} is a tuple $(\mathcal{C}_x, \mathcal{D}_y)$ where $\mathcal{C}_x \subseteq \mathcal{X}$ and $\mathcal{D}_y(\mathbf{x})$ is a distribution over \mathcal{Y} . (That is, \mathcal{D}_y , like \mathcal{C}_y , is a partial function well-defined on \mathcal{C}_x .) \mathcal{C} is ϵ -*satisfied* by a BNN with prior $\mathbf{W} \sim p(\mathbf{w})$ if, $\forall \mathbf{x} \in \mathcal{C}_x$ and for some $\epsilon \in [0, 1]$:

$$D_{DIV}\left(p(\Phi_{\mathbf{W}} | \mathbf{x}) \parallel \mathcal{D}_y(\mathbf{x})\right) \leq \epsilon \quad (2)$$

where D_{DIV} is any valid measure of divergence between two distributions over \mathcal{Y} .

We seek to construct a prior $\mathbf{W} \sim p(\mathbf{w})$ such that the BNN ϵ -satisfies, for some small ϵ , a specified constraint \mathcal{C} . An intuitive way to connect a prior in parameter space to \mathcal{C} (defined in *function* space) is to evaluate how well the implicit distribution of $\Phi_{\mathbf{W}}$, induced by the distribution of \mathbf{W} , satisfies \mathcal{C} . In Section 4.1, we construct a prior that is conditioned on \mathcal{C} and explicitly factors in the likelihood $p(\mathcal{C} | \mathbf{w})$ of constraint satisfaction. In Section 4.3, we present an amortized variant by performing variational optimization on objectives (1) or (2) directly.

4.1 Conditional Output-Constrained Prior

A fully Bayesian approach requires a proper distribution that describes how well any $\mathbf{w} \in \mathcal{W}$ satisfies \mathcal{C} by way of $\Phi_{\mathbf{w}}$. Informally, this distribution must be conditioned on *all* $\mathbf{x} \in \mathcal{C}_x$ (though we sample finitely during inference) and is the “product” of how well $\Phi_{\mathbf{w}}(\mathbf{x})$ satisfies \mathcal{C} for *each* $\mathbf{x} \in \mathcal{C}_x$. This notion can be formalized by defining \mathcal{C} as a stochastic process indexed on \mathcal{C}_x .

Let $\mathbf{x} \in \mathcal{C}_x$ be any single input. In measure-theoretic terms, the corresponding output $Y : \Omega \rightarrow \mathcal{Y}$ is defined on some probability space $(\Omega, \mathcal{F}, \mathbf{P}_{g, \mathbf{x}})$, where Ω and \mathcal{F} are the typical sample space and σ -algebra, and $\mathbf{P}_{g, \mathbf{x}}$ is any valid probability measure corresponding to a distribution $p_g(\cdot | \mathbf{x})$ over \mathcal{Y} . Then $(\Omega, \mathbf{F}, \mathbf{P}_g)$ is the joint probability space, where $\Omega = \prod_{\mathbf{x} \in \mathcal{C}_x} \Omega$, \mathbf{F} is the product σ -algebra and $\mathbf{P}_g = \prod_{\mathbf{x} \in \mathcal{C}_x} \mathbf{P}_{g, \mathbf{x}}$ is the product measure (a pushforward measure from $\mathbf{P}_{g, \mathbf{x}}$). Let $\mathcal{C}\mathcal{P} : \Omega \rightarrow \mathcal{Y}^{\mathcal{C}_x}$ be the stochastic process indexed by \mathcal{C}_x , where $\mathcal{Y}^{\mathcal{C}_x}$ denotes the set of all measurable functions from \mathcal{C}_x into \mathcal{Y} . The law of the process $\mathcal{C}\mathcal{P}$ is $p(S) = \mathbf{P}_g \circ \mathcal{C}\mathcal{P}^{-1}(S)$ for all $S \in \mathcal{Y}^{\mathcal{C}_x}$. For any finite subset $\{Y^{(1)}, \dots, Y^{(T)}\} \subseteq \mathcal{C}\mathcal{P}$ indexed by $\{\mathbf{x}^{(1)}, \dots, \mathbf{x}^{(T)}\} \subseteq \mathcal{C}_x$,

$$p(Y^{(1)} = y^{(1)}, \dots, Y^{(T)} = y^{(T)}) = \prod_{t=1}^T p_g(Y^{(t)} = y^{(t)} | \mathbf{x}^{(t)}) \quad (3)$$

$\mathcal{C}\mathcal{P}$ is a valid stochastic process as it satisfies both (finite) exchangeability and consistency, which are sufficient conditions via the Kolmogorov Extension Theorem [23]. As the BNN output $\Phi_{\mathbf{w}}(\mathbf{x})$ can be evaluated for all $\mathbf{x} \in \mathcal{C}_x$ and $\mathbf{w} \in \mathcal{W}$, $\mathcal{C}\mathcal{P}$ allows us to formally describe how much $\Phi_{\mathbf{w}}$ satisfies \mathcal{C} , by determining the measure of the realization $\Phi_{\mathbf{w}}^{\mathcal{C}_x} \in \mathcal{Y}^{\mathcal{C}_x}$.

Definition 4.4. Let \mathcal{C} be any (deterministic or probabilistic) constraint and \mathcal{CP} the stochastic process defined on $\mathcal{Y}^{\mathcal{C}_x}$ for some measure \mathbf{P}_g . The **conditional output-constrained prior (COCP)** on \mathbf{W} is defined as

$$p_{\mathcal{C}}(\mathbf{w}) = p_f(\mathbf{w})p(\Phi_{\mathbf{w}}^{\mathcal{C}_x}) \quad (4)$$

where $p_f(\mathbf{w})$ is any distribution on \mathbf{W} that is independent of \mathcal{C} , and $\Phi_{\mathbf{w}}^{\mathcal{C}_x} \in \mathcal{Y}^{\mathcal{C}_x}$ is the realization of \mathcal{CP} corresponding to the BNN output $\Phi_{\mathbf{w}}(\mathbf{x})$ for all $\mathbf{x} \in \mathcal{C}_x$.

We can view (4) loosely as an application of Bayes' Rule, where the realization $\Phi_{\mathbf{w}}^{\mathcal{C}_x}$ of the stochastic process \mathcal{CP} is the evidence (likelihood) of \mathcal{C} being satisfied by \mathbf{w} and $p_f(\mathbf{w})$ is the unconditional prior over \mathcal{W} . This implies that the posterior that we are ultimately inferring is $\mathbf{W}|D_{tr}, \mathcal{CP}$, i.e. with extra conditioning on \mathcal{CP} . To ease the burden on notation, we will drop the explicit conditioning on \mathcal{CP} and treat $p_{\mathcal{C}}(\mathbf{w})$ as the unconditional prior over \mathcal{W} . To make clear the presence of \mathcal{C} , we will denote the constrained posterior as $p_{\mathcal{C}}(\mathbf{w}|D_{tr})$. Definition 4.4 generalizes to multiple constraints $\mathcal{C}^{(1)}, \dots, \mathcal{C}^{(m)}$ by conditioning on all $\mathcal{C}^{(i)}$ and evaluating $\Phi_{\mathbf{w}}$ for each constraint. Assuming the constraints to be mutually independent, $p_{\mathcal{C}^{(1)}, \dots, \mathcal{C}^{(m)}}(\mathbf{w}) = p_f(\mathbf{w}) \prod_{i=1}^m p(\Phi_{\mathbf{w}}^{\mathcal{C}^{(i)}})$.

It remains to describe what measure \mathbf{P}_g we should choose such that $p(\Phi_{\mathbf{w}}^{\mathcal{C}_x})$ is a likelihood distribution that faithfully evaluates the extent to which \mathcal{C} is satisfied. For probabilistic output constraints, we simply set $p_g(\cdot|\mathbf{x})$ to be $\mathcal{D}_y(\mathbf{x})$. For deterministic output constraints, we propose a number of distributions over \mathcal{Y} that corresponds well to \mathcal{C}_y , the set of permitted (or excluded) output values.

Example: Positive Mixture of Gaussian Constraint A positive constraint \mathcal{C}^+ for regression, where $\mathcal{C}_y(\mathbf{x}) = \{y_1, \dots, y_K\}$ contains multiple values, corresponds to the situation wherein the expert knows potential ground-truth values over \mathcal{C}_x . A natural choice is the Gaussian mixture model: $\mathcal{CP}(\mathbf{x}) \sim \sum_{k=1}^K \omega_k \mathcal{N}(y_k, \sigma_c^2)$, where σ_c is the standard deviation of the Gaussian, a hyperparameter controlling the strictness of \mathcal{C} satisfaction, and ω_k are the mixing weights: $\sum_{k=1}^K \omega_k = 1$.

Example: Positive Dirichlet Constraint For K -classification, the natural distribution to consider is the Dirichlet distribution, whose support (the standard K -simplex) corresponds to the K -tuple of predicted probabilities on all classes. For a positive constraint \mathcal{C}^+ , we specify:

$$\mathcal{CP}(\mathbf{x}) \sim \text{Dir}(\boldsymbol{\alpha}); \quad \boldsymbol{\alpha}_i = \begin{cases} \gamma & \text{if } i \in \mathcal{C}_y(\mathbf{x}) \\ \gamma(1-c) & \text{otherwise} \end{cases} \quad \text{where } \gamma \geq 1, 0 < c < 1 \quad (5)$$

Example: Negative Exponential Constraint A negative constraint \mathcal{C}^- for regression takes $\mathcal{C}_y(\mathbf{x})$ to be the set of values that cannot be the output of \mathbf{x} . For the case where \mathcal{C}_y is determined from a set of inequalities of the form $\{g_1(\mathbf{x}, y) \leq 0, \dots, g_l(\mathbf{x}, y) \leq 0\}$, where *obeying all* inequalities implies that $y \in \mathcal{C}_y(\mathbf{x})$ and hence \mathcal{C}^- is *not satisfied*, we can consider an exponential distribution that penalizes y based on how each inequality is violated:

$$p_g(\mathcal{CP}(\mathbf{x}) = y'|\mathbf{x}) \propto \exp \left\{ -\gamma \cdot \prod_{i=1}^l \sigma_{\tau_0, \tau_1}(g_i(\mathbf{x}, y')) \right\} \quad (6)$$

where $\sigma_{\tau_0, \tau_1}(z) = \frac{1}{4}(\tanh(-\tau_0 z) + 1)(\tanh(-\tau_1 z) + 1)$ and γ is a decay hyperparameter. The sigmoidal function $\sigma_{\tau_0, \tau_1}(g_i(\mathbf{x}, y'))$ is a soft indicator of whether $g_i \leq 0$ is satisfied. $p_g(\mathcal{CP}(\mathbf{x}) = y'|\mathbf{x})$ is small if every $g_i(\mathbf{x}, y') \leq 0$, i.e. all inequalities are obeyed and \mathcal{C}^- is violated.

4.2 Inference with COCPs

A complete specification of (4) is sufficient for inference using COCPs, as the expression $p_{\mathcal{C}}(\mathbf{w})$ can simply be substituted for that of $p(\mathbf{w})$ in all black-box BNN inference algorithms. Since (4) cannot be computed exactly due to the intractability of $p(\Phi_{\mathbf{w}}^{\mathcal{C}_x})$ for uncountable \mathcal{C}_x , we will draw a finite sample $\{\mathbf{x}^{(t)}\}_{t=1}^T$ of $\mathbf{x} \in \mathcal{C}_x$ (e.g. uniformly across \mathcal{C}_x or Brownian sampling if \mathcal{C}_x is unbounded) at the start of the inference process and compute (3) as an estimator of $p(\Phi_{\mathbf{w}}^{\mathcal{C}_x})$ instead:

$$\tilde{p}_{\mathcal{C}}(\mathbf{w}) = p_f(\mathbf{w}) \prod_{t=1}^T p_g(\Phi_{\mathbf{w}}(\mathbf{x}^{(t)})|\mathbf{x}^{(t)}) \quad (7)$$

The computational runtime of COCPs increases with the input dimensionality Q and the size of \mathcal{C}_x . However, we note that many sampling techniques from statistical literature can be applied to COCPs in lieu of naive uniform sampling. We use the isotropic Gaussian prior for $p_f(\mathbf{w})$.

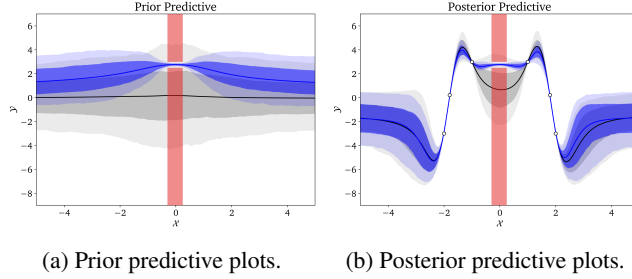


Figure 1: 1D regression with the negative constraint: $\mathcal{C}_x^- = [-0.3, 0.3]$ and $\mathcal{C}_y^- = (-\infty, 2.5] \cup [3, \infty)$, in red. The negative exponential COCP (6) is used. Even with such a restrictive constraint, the predictive uncertainty of the OC-BNN (blue) drops sharply to fit within the permitted region of \mathcal{Y} . Note that the OC-BNN posterior uncertainty matches the baseline (gray) everywhere except near \mathcal{C}_x .

Absolute guarantees of (1) or (2), i.e. achieving $\epsilon = 0$, are necessary in certain applications but challenging for COCPs. Zero-variance or truncated $p_{\mathcal{C}}(\mathbf{w})$, as means of ensuring hard constraint satisfaction, are theoretically plausible but numerically unstable for BNN inference, particularly gradient-based methods. Nevertheless, as modern inference algorithms produce finite approximations of the true posterior, practical guarantees can be imposed, such as via further rejection sampling on top of the constrained posterior $p_{\mathcal{C}}(\mathbf{w}|D_{tr})$. We demonstrate in Section 5 that unlike naive rejection sampling from $p(\mathbf{w}|D_{tr})$, doing so from $p_{\mathcal{C}}(\mathbf{w}|D_{tr})$ is both tractable and practical for ensuring zero constraint violations.

4.3 An Amortized Output-Constrained Prior

Instead of constructing a PDF over \mathbf{w} explicitly dependent on $\Phi_{\mathbf{w}}$ and \mathcal{C} , we can learn a variational approximation $q_{\lambda}(\mathbf{w})$ where we optimize λ directly with respect to our goals, (1) or (2). As both objectives contain an intractable expectation over \mathbf{W} , we seek a closed-form approximation of the variational prior predictive $p_{\lambda}(\Phi_{\mathbf{W}}|\mathbf{x})$. For the regression and *binary* classification settings, there are well-known approximations, which we state in Appendix B as (17) and (21) respectively. Our objectives are:

$$\lambda^* = \arg \max_{\lambda \in \Lambda} \int_{\mathcal{Y}} \mathbb{I}[y \circ \mathcal{C}_y(\mathbf{x})] \cdot p_{\lambda}(\Phi_{\mathbf{W}} = y|\mathbf{x}) dy \quad (8)$$

$$\lambda^* = \arg \min_{\lambda \in \Lambda} D_{DIV} \left(p_{\lambda}(\Phi_{\mathbf{W}}|\mathbf{x}) \parallel \mathcal{D}_y(\mathbf{x}) \right) \quad (9)$$

As (8) and (9) are defined for a specific $\mathbf{x} \in \mathcal{C}_x$, we need to stochastically optimize over all $\mathbf{x} \in \mathcal{C}_x$. Even though (8) is still an integral over \mathcal{Y} , it is tractable since we only need to compute the CDF corresponding to the boundary elements of \mathcal{C}_y . We denote the resulting learnt distribution $q_{\lambda^*}(\mathbf{w})$ as the **amortized output-constrained prior (AOCP)**. Unlike COCPs, where $p_{\mathcal{C}}(\mathbf{w})$ is directly evaluated during posterior inference, we first perform optimization to learn λ^* , which can then be used for inference independently over any number of training tasks (datasets) D_{tr} .

5 Low-Dimensional Simulations

COCPs and AOCPs are conceptually simple but work well, even on non-trivial output constraints. As a proof-of-concept, we simulate toy data and constraints for small input dimension and visualize the predictive distributions. See Appendix C for experimental details.

OC-BNNs model uncertainty in a manner that respects constrained regions and explains training data, without making overconfident predictions outside \mathcal{C}_x . Figure 1 shows the prior and posterior predictive plots for a negative constraint for regression, where a highly restrictive constraint was intentionally chosen. Unlike the naive baseline BNN, the OC-BNN satisfies the constraint, with its predictive variance smoothly narrowing as \mathbf{x} approaches \mathcal{C}_x so as to be entirely confined within $\mathcal{Y} - \mathcal{C}_y$. After posterior inference, the OC-BNN fits all data points in D_{tr} closely while still respecting the constraint. Far from \mathcal{C}_x , the OC-BNN is not overconfident, maintaining a wide variance like the baseline. Figure 2 shows an analogous example for classification. Similarly, the OC-BNN fits the data and respects the constraint within \mathcal{C}_x , without showing a strong preference for any class OOD.

OC-BNNs can capture global input-output relationships between \mathcal{X} and \mathcal{Y} , subject to sampling efficacy. Figure 3a shows an example where we enforce the constraint $xy \geq 0$. Even though the

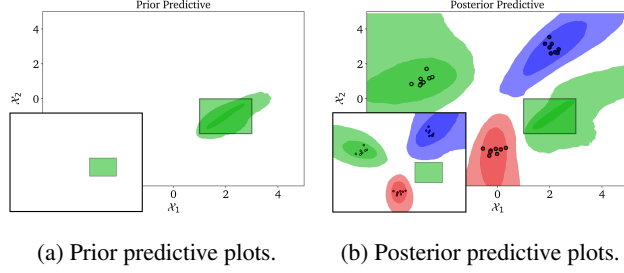


Figure 2: 2D 3-classification with the positive constraint: $\mathcal{C}_x^+ = (1, 3) \times (-2, 0)$ and $\mathcal{C}_y^+ = \{\text{green}\}$. The main plots are the OC-BNN predictives; insets are the baselines. Input region is shaded by the predicted class if above a threshold certainty. The positive Dirichlet COCP (5) is used. In both the prior and posterior, the constrained region (green rectangle) enforces the prediction of the green class.

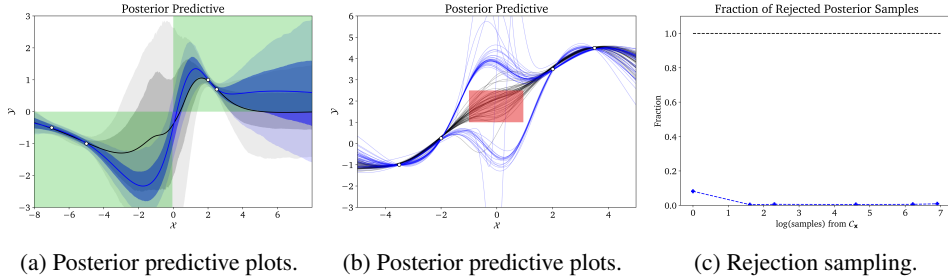


Figure 3: (a) 1D regression with the positive constraint: $\mathcal{C}_x^+ = \mathbb{R}$ and $\mathcal{C}_y^+(\mathbf{x}) = \{y \mid \mathbf{x} \cdot y \geq 0\}$ (green), using AOCP. (b) 1D regression with the negative constraint: $\mathcal{C}_x^- = [-1, 1]$ and $\mathcal{C}_y^- = [1, 2.5]$ (red), with the negative exponential COCP (6). The 50 SVGD particles represent functions passing above and below the constrained region, capturing two distinct predictive modes. (c) Fraction of rejected SVGD particles (out of 100) for the OC-BNN (blue, plotted as a function of log-samples used with COCP) and the baseline (black). All baseline particles were rejected, however, only 4% of particles were rejected, using just only 5 COCP samples.

training data itself adheres to this constraint, learning from D_{tr} alone is insufficient. The OC-BNN posterior predictive narrows significantly (compared to the baseline) to fit the constraint, particularly near $x = 0$. Note, however, that OC-BNNs can only learn as well as sampling from \mathcal{C}_x permits.

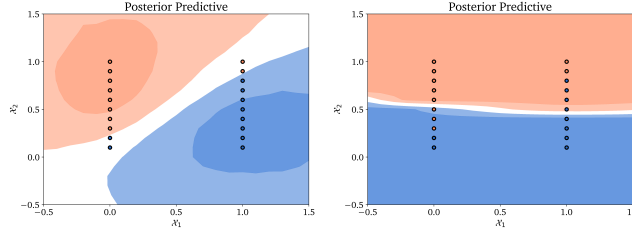
OC-BNNs can capture posterior multimodality. As NNs are highly expressive, BNN posteriors can contain multiple modes of significance. In Figure 3b, the negative constraint is specified in such a way as to allow for functions that fit D_{tr} to pass both above or below the constrained region. Accordingly, the resulting OC-BNN posterior predictive contains significant probability mass on either side of \mathcal{C}_y . Importantly, note that the negative exponential COCP does not *explicitly* indicate the presence of multiple modes, showing that OC-BNNs naturally facilitate mode exploration.

OC-BNNs can model interpretable desiderata represented as output constraints. OC-BNNs can be used to enforce important qualities that the system should possess. Figure 4 demonstrates a fairness constraint known as **demographic parity**:

$$p(Y = 1 | \mathbf{x}_A = 1) = p(Y = 1 | \mathbf{x}_A = 0) \quad (10)$$

where \mathbf{x}_A is a protected attribute such as race or gender. (10) is expressed as a probabilistic output constraint. The OC-BNN not only learns to respect this constraint, it does so in the presence of *conflicting training data* (D_{tr} is an unfair dataset).

Sensitivity to Inference and Conflicting Data Figure 5 in Appendix D shows the same negative constraint used in Figure 1, except using different inference algorithms. There is little difference in these predictive plots besides the idiosyncrasies unique to each algorithm. Hence **OC-BNNs behave reliably on, and are agnostic to, all major classes of BNN inference.** If \mathcal{C} and D_{tr} are incompatible, such as with adversarial or biased data, the posterior depends on (i) model capacity and (ii) factors affecting the prior and likelihood, e.g. volume of data or OC-BNN hyperparameters. For example, Figure 6 in Appendix D shows a BNN with enough capacity to fit both the noisy data



(a) Baseline posterior predictive. (b) OC-BNN posterior predictive.

Figure 4: 2D binary classification. Suppose a hiring task where \mathcal{X}_1 (binary) indicates membership of a protected trait (e.g. gender or race) and \mathcal{X}_2 denotes skill level. Hence a positive (orange) classification should be correlated with higher values of \mathcal{X}_2 . The dataset D_{tr} displays historic bias, where members of the protected class ($x_1 = 1$) are discriminated against ($Y = 1$ iff $x_1 = 1, x_2 \geq 0.8$, but $Y = 1$ iff $x_1 = 0, x_2 \geq 0.2$). A naive BNN (a) would learn an unfair linear separator. However, learning the probabilistic constraint: $\mathcal{D}_y(\mathbf{x})$ as the distribution where $p(\Phi(\mathbf{x}) = 1) = x_2$ with the AOCP allows the OC-BNN (b) to learn a fair separator, **despite a biased dataset**.

as well as ground-truth constraints, resulting in “overfitting” of the posterior predictive. However, the earlier example in Figure 4 prioritizes the fairness constraint, as the small size of D_{tr} constitutes weaker evidence.

Ensuring Hard Constraints using Rejection Sampling A few SVGD particles in Figure 3b violate the constraint. While COCPs cannot guarantee $\epsilon = 0$ satisfaction, hard constraints can be *practically* enforced. Consider the idealized, truncated predictive distributions of the baseline BNN and OC-BNN, whereby for each $\mathbf{x} \in \mathcal{C}_x$, we set $p(Y = y|\mathbf{x}) = 0$ where the constraint is violated and normalize the remaining density to 1. These distributions represent zero constraint violation (by definition) and can be obtained via rejection sampling from the baseline BNN or OC-BNN posteriors. Figure 3c shows the results of performing such rejection sampling, using the same setup as Figure 3b. As shown, rejection sampling is intractable for the baseline BNN (not a single SVGD particle accepted), but works well on the OC-BNN, even when using only a small sample count from \mathcal{C}_x to compute $p_C(\mathbf{w})$. This experiment shows not only that naive rejection sampling (on ordinary BNNs) to weed out posterior constraint violation is futile, but also that *doing the same on OC-BNNs* is a practical workaround to ensure that hard constraints are satisfied, which is generally difficult to achieve in ideal, probabilistic settings.

6 Experiments with Real-World Data

To demonstrate the efficacy of OC-BNNs, we apply meaningful and interpretable output constraints on real-life datasets. As our method is the first such work for BNN classification, the baseline that we compare our results to is an ordinary BNN with the isotropic Gaussian prior. Experimental details for all three applications can be found in Appendix C.

6.1 Application: Clinical Action Prediction

	Train		Test		
	Accuracy	F_1 Score	Accuracy	F_1 Score	Constraint Violation
BNN	0.713	0.548	0.738	0.222	0.783
OC-BNN	0.735	0.565	0.706	0.290	0.136

Table 1: Compared to the baseline, the OC-BNN maintains equally high accuracy and F_1 score on both train and test sets. The violation fraction decreased about six-fold when using OC-BNNs.

The MIMIC-III database [12] contains physiological features of intensive care unit patients. We construct a dataset ($N = 405K$) of 8 relevant features and consider a binary classification task of whether clinical interventions for hypotension management — namely, vasopressors or IV fluids — should be taken for any patient. We specify two **physiologically feasible**, positive (deterministic) constraints: (1) if the patient has high creatinine, high BUN and low urine, then action should be taken ($\mathcal{C}_y = \{1\}$); (2) if the patient has high lactate and low bicarbonate, action should also be taken. The positive Dirichlet COCP (5) is used. In addition to **accuracy** and **F_1 score** on the test

		with race feature		without race feature	
		BNN	OC-BNN	BNN	OC-BNN
Train	Accuracy	0.837	0.708	0.835	0.734
	F_1 Score	0.611	0.424	0.590	0.274
	African American High-Risk Fraction	0.355	0.335	0.309	0.203
	Non-African American High-Risk Fraction	0.108	0.306	0.123	0.156

Table 2: The OC-BNN predicts both racial groups with almost equal rates of high-risk recidivism, compared to a $3.5\times$ difference on the baseline. However, accuracy metrics decrease (expectedly).

set ($N = 69\text{K}$), we also measure ϵ -satisfaction on the constraints as **violation fraction**, where we sample 5K points in \mathcal{C}_x and measure the fraction of those points violating either constraint.

Results Table 1 summarizes the experimental results. The main takeaway is that **OC-BNNs maintain classification accuracy while reducing constraint violations**. The results show that OC-BNNs match standard BNNs on all predictive accuracy metrics, while satisfying the constraints to a far greater extent. This is because the constraints are intentionally specified in input regions out-of-distribution, and hence incorporating this knowledge augments what the OC-BNN learns from D_{tr} alone. This experiment affirms the low-dimensional simulations in Section 5, showing that OC-BNNs are able to obey interpretable constraints without sacrificing predictive power.

6.2 Application: Recidivism Prediction

COMPAS is a proprietary model, used by the United States criminal justice system, that scores criminal defendants on their risk of recidivism. A study by ProPublica in 2016 found it to be racially biased against African American defendants [1, 16]. We use the same dataset as this study, containing 9 features on $N = 6172$ defendants related to their criminal history and demographic attributes. We consider the same binary classification task as in Slack et al. [24] — predicting whether a defendant is profiled by COMPAS as being high-risk. We specify the **fairness** constraint that the probability of predicting high-risk recidivism should not depend on race: for all ($\mathcal{C}_x = \mathbb{R}^9$) individuals, the high-risk probability should be identical to their actual recidivism history (\mathcal{D}_y is such that $p(y = 1) = \text{two_year_recid}$). The AOCP is used. D_{tr} is incompatible with this constraint since COMPAS itself demonstrates racial bias. We train on two versions of D_{tr} — with/without the inclusion of race as an explicit feature. As the dataset is small and imbalanced, we directly evaluate the training set. To measure ϵ -satisfaction, we report the **fraction of the sensitive attribute** (African American defendants vs. non-African American defendants) predicted as high-risk recidivists.

Results Table 2 summarizes the results. By constraining recidivism prediction to the defendant’s actual criminal history, **OC-BNNs strictly enforce a fairness constraint**. On both versions of D_{tr} , the baseline BNN predicts unequal risk for the two groups since the output labels (COMPAS decisions) are themselves biased. This inequality is more stark when the race feature is included, as the model learns the explicit, positive correlation between race and the output label. For both datasets, the fraction of the two groups being predicted as high-risk recidivists equalized after imposing the constraint using OC-BNNs. Unlike the previous example, OC-BNNs have lower predictive accuracy on D_{tr} than standard BNNs. This is *expected* since the training dataset is biased, and enforcing racial fairness comes at the expense of correctly predicting biased labels.

6.3 Application: Credit Scoring Prediction

Young adults tend to be disadvantaged by credit scoring models as their lack of credit history results in them being poorly represented by data (see e.g. [14]). We consider the Give Me Some Credit dataset ($N = 133\text{K}$) [13], containing binary labels on whether individuals will experience impending financial distress, along with 10 features related to demographics and financial history. Motivated by Ustun et al. [26]’s work on *recourse* (defined as the extent that input features must be altered to change the model’s outcome), we consider the feature `RevolvingUtilizationOfUnsecuredLines` (RUUL), which has a ground-truth positive correlation with financial distress. We analyze how much a young adult under 35 has to reduce RUUL to flip their prediction to negative in three cases: (i) a BNN trained on the full dataset, (ii) a BNN trained on a blind dataset ($\text{age} \geq 35$), (iii) an OC-BNN with an **actionability constraint**: for young adults, predict “no financial distress” even if RUUL is large. The positive Dirichlet COCP (5) is used. In addition to scoring accuracy and F_1 score on the entire test set ($N = 10\text{K}$); we measure the **effort of recourse** as the mean difference of RUUL between the two outcomes ($\hat{Y} = 0$ or 1) on the subset of individuals where $\text{age} < 35$ ($N = 1.5\text{K}$).

Results As can be seen in Table 3, the ground-truth positive correlation between RUJL and the output is weak, and the effort of recourse is consequentially low. However, the baseline BNN naturally learns a stronger correlation, resulting in a higher effort of recourse. This effect is amplified if the BNN is trained on a limited dataset *without* data on young adults. When an actionability constraint is enforced, the OC-BNN **reduces the effort of recourse without sacrificing predictive accuracy** on the test set, reaching the closest to the ground-truth recourse.

		Ground Truth	BNN (Full)	BNN (Blind)	OC-BNN
Test	Accuracy		0.890	0.871	0.895
	F_1 Score		0.355	0.346	0.350
	Effort of Recourse	0.287	0.419	0.529	0.379

Table 3: All three models have comparable accuracy on the test set. However, the OC-BNN has the lowest recourse effort (closest to ground truth).

7 Discussion

The usage of OC-BNNs depends on how we view constraints in relation to data. The clinical action prediction and credit scoring tasks are cases where the constraint is a complementary source of information, being defined in input regions where D_{tr} is sparse. The recidivism prediction task represents the paradigm where D_{tr} is inconsistent with the constraint, which serves to correct an existing bias. Both approaches are fully consistent with the Bayesian framework, whereby coherent inference decides how the likelihood and prior effects each shape the resulting posterior.

In contrast with [7, 19, 25], **OC-BNNs take a sampling-based approach to bridge functional and parametric objectives.** The simplicity of this can be advantageous — output constraints are a common currency of knowledge easily specified by domain experts, in contrast to more technical forms such as stochastic process priors. While effective sampling is a prerequisite for accurate inference, we note that the sampling complexity of OC-BNNs is tractable even at the dimensionality we consider in Section 6. Note that we sample in \mathcal{X} -space, which is much smaller than \mathcal{W} -space.

OC-BNNs are intuitive to formulate and work well in real-life settings. Even though COCPs and AOCPs echo well-known notions of data-based regularization, it is not immediately clear that these ideas are effectual in practice, and lead to well-behaved posteriors with appropriate output variance (both within and without constrained regions). Our work represents the first such effort (i) to create a broad framework for reasoning with diverse forms of output constraints, and (ii) that solidly demonstrates its utility on a corresponding range of real-life applications.

8 Conclusion

We propose OC-BNNs, which allow us to incorporate interpretable and intuitive prior knowledge, in the form of output constraints, into BNNs. Through a series of low-dimensional simulations as well as real-world applications with realistic constraints, we show that OC-BNNs generally maintain the desirable properties of ordinary BNNs while satisfying specified constraints. OC-BNNs complement a nascent strand of research that aims to incorporate rich and informative functional beliefs into deep Bayesian models. Our work shows promise in various high-stakes domains, such as healthcare and criminal justice, where both uncertainty quantification and prior expert constraints are necessary for safe and desirable model behavior.

Broader Impact

Our work incorporates task-specific domain knowledge, in the form of output constraints, into BNNs. We wish to highlight two key positive impacts. **(1)** OC-BNNs allow us to manipulate an **interpretable** form of knowledge. They can be useful even to domain experts without technical machine learning expertise, who can easily specify such constraints for model behavior. A tool like this can be used alongside experts in the real world, such as physicians or judges. **(2)** Bayesian models like BNNs and OC-BNNs are typically deployed in “high-stakes” domains, which include those with societal impact. We intentionally showcase **applications of high societal relevance**, such as recidivism prediction and credit scoring, where the ability to specify and satisfy constraints can lead to fairer and more ethical model behavior.

That being said, there are considerations and limitations. (1) If the model capacity is low (e.g. the BNN is small), constraints and model capacity may interact in unexpected ways that are not transparent to the domain expert. (2) Our sampling approach allows us to be very general in specifying constraints, but it also creates a trade-off between computational efficiency and accuracy of constraint enforcement. (3) Finally, the expert could mis-specify or even maliciously specify constraints. The first two considerations can be mitigated by careful optimization and robustness checks; the latter by making the constraints public and reviewable by others.

Acknowledgments and Disclosure of Funding

The authors are grateful to Srivatsan Srinivasan, Anirudh Suresh, Jiayu Yao and Melanie F. Pradier for contributions to an initial version of this work [28], as well as Gerald Lim, M.B.B.S. for helpful discussions on the clinical action prediction task. HL acknowledges support from Google. WY and FDV acknowledge support from the Sloan Foundation.

References

- [1] Julia Angwin, Jeff Larson, Surya Mattu, and Lauren Kirchner. Machine Bias: Risk Assessments in Criminal Sentencing. *ProPublica*, 2016.
- [2] Cem Anil, James Lucas, and Roger Grosse. Sorting Out Lipschitz Function Approximation. In *Proceedings of the 36th International Conference on Machine Learning*, 2019.
- [3] Christopher M Bishop. *Pattern Recognition and Machine Learning*. Springer, 2006.
- [4] Charles Blundell, Julien Cornebise, Koray Kavukcuoglu, and Daan Wierstra. Weight Uncertainty in Neural Networks. In *Proceedings of the 32nd International Conference on Machine Learning*, 2015.
- [5] Simon Duane, Anthony D Kennedy, Brian J Pendleton, and Duncan Roweth. Hybrid Monte Carlo. *Physics Letters B*, 195(2):216–222, 1987.
- [6] John Duchi, Elad Hazan, and Yoram Singer. Adaptive Subgradient Methods for Online Learning and Stochastic Optimization. *Journal of Machine Learning Research*, 12(Jul):2121–2159, 2011.
- [7] Marta Garnelo, Jonathan Schwarz, Dan Rosenbaum, Fabio Viola, Danilo J Rezende, S.M. Ali Eslami, and Yee Whye Teh. Neural Processes. In *35th ICML Workshop on Theoretical Foundations and Applications of Deep Generative Models*, 2018.
- [8] Alex Graves. Practical Variational Inference for Neural Networks. In *Advances in Neural Information Processing Systems*, pages 2348–2356, 2011.
- [9] Danijar Hafner, Dustin Tran, Timothy Lillicrap, Alex Irpan, and James Davidson. Noise Contrastive Priors for Functional Uncertainty. *arXiv:1807.09289*, 2018.
- [10] Geoffrey E Hinton and Drew Van Camp. Keeping the Neural Networks Simple by Minimizing the Description Length of the Weights. In *Proceedings of the 6th Annual Conference on Computational Learning Theory*, pages 5–13, 1993.
- [11] Kurt Hornik, Maxwell Stinchcombe, and Halbert White. Multilayer Feedforward Networks are Universal Approximators. *Neural Networks*, 2(5):359–366, 1989.
- [12] Alistair EW Johnson, Tom J Pollard, Lu Shen, H Lehman Li-wei, Mengling Feng, Mohammad Ghassemi, Benjamin Moody, Peter Szolovits, Leo Anthony Celi, and Roger G Mark. MIMIC-III, A Freely Accessible Critical Care Database. *Scientific Data*, 3:160035, 2016.
- [13] Kaggle. Give Me Some Credit. <http://www.kaggle.com/c/GiveMeSomeCredit/>, 2011.
- [14] Nathan Kallus and Angela Zhou. Residual Unfairness in Fair Machine Learning from Prejudiced Data. In *Proceedings of the 35th International Conference on Machine Learning*, 2018.
- [15] Diederik P Kingma and Max Welling. Auto-Encoding Variational Bayes. In *Proceedings of the 2nd International Conference on Learning Representations*, 2014.

- [16] Jeff Larson, Surya Mattu, Lauren Kirchner, and Julia Angwin. How We Analyzed the COMPAS Recidivism Algorithm. *ProPublica*, 2016.
- [17] Qiang Liu and Dilin Wang. Stein Variational Gradient Descent: A General Purpose Bayesian Inference Algorithm. In *Advances in Neural Information Processing Systems*, pages 2378–2386, 2016.
- [18] Marco Lorenzi and Maurizio Filippone. Constraining the Dynamics of Deep Probabilistic Models. In *Proceedings of the 35th International Conference on Machine Learning*, 2018.
- [19] Christos Louizos, Xiahan Shi, Klamer Schutte, and Max Welling. The Functional Neural Process. In *Advances in Neural Information Processing Systems*, pages 8743–8754, 2019.
- [20] David J C MacKay. Probable Networks and Plausible Predictions — a Review of Practical Bayesian Methods for Supervised Neural Networks. *Network: Computation in Neural Systems*, 6(3):469–505, 1995.
- [21] Radford M Neal. *Bayesian Learning for Neural Networks*. PhD thesis, University of Toronto, 1995.
- [22] Radford M Neal. MCMC Using Hamiltonian Dynamics. *Handbook of Markov Chain Monte Carlo*, 2(11):2, 2011.
- [23] Bernt Øksendal. Stochastic Differential Equations. In *Stochastic Differential Equations*, pages 65–84. Springer, 2003.
- [24] Dylan Slack, Sophie Hilgard, Emily Jia, Sameer Singh, and Himabindu Lakkaraju. Fooling LIME and SHAP: Adversarial Attacks on Post hoc Explanation Methods. In *Proceedings of the 3rd AAAI/ACM Conference on Artificial Intelligence, Ethics, and Society*, pages 180–186, 2020.
- [25] Shengyang Sun, Guodong Zhang, Jiaxin Shi, and Roger Grosse. Functional Variational Bayesian Neural Networks. In *Proceedings of the 7th International Conference on Learning Representations*, 2019.
- [26] Berk Ustun, Alexander Spangher, and Yang Liu. Actionable Recourse in Linear Classification. In *Proceedings of the ACM Conference on Fairness, Accountability and Transparency*, pages 10–19, 2019.
- [27] Andrew Gordon Wilson. The Case for Bayesian Deep Learning. *arXiv:2001.10995*, 2020.
- [28] Wanqian Yang, Lars Lorch, Moritz A Graule, Srivatsan Srinivasan, Anirudh Suresh, Jiayu Yao, Melanie F Pradier, and Finale Doshi-Velez. Output-Constrained Bayesian Neural Networks. In *36th ICML Workshop on Uncertainty and Robustness in Deep Learning*, 2019.
- [29] Seungil You, David Ding, Kevin Canini, Jan Pfeifer, and Maya Gupta. Deep Lattice Networks and Partial Monotonic Functions. In *Advances in Neural Information Processing Systems*, pages 2981–2989, 2017.

A Bayesian Inference over Neural Networks

On a supervised model parameterized by \mathbf{W} , we seek to infer the conditional distribution $\mathbf{W}|D_{tr}$, which can be computed from the data D_{tr} using **Bayes' Rule**:

$$p(\mathbf{w}|D_{tr}) = \frac{p(\mathbf{w})p(D_{tr}|\mathbf{w})}{p(D_{tr})} \quad (11)$$

We call $p(\mathbf{w}|D_{tr})$ the **posterior** (distribution), $p(\mathbf{w})$ the **prior** (distribution) and $p(D_{tr}|\mathbf{w})$ the **likelihood** (distribution)¹. Since D_{tr} is i.i.d. by assumption, we can decompose the likelihood into individual observations:

$$p(D_{tr}|\mathbf{w}) = \prod_{i=1}^N p(Y_i|\mathbf{x}_i, \mathbf{w}) \quad (12)$$

The prior and likelihood are both modelling choices. The evidence probability $p(D_{tr})$ is an intractable integral

$$p(D_{tr}) = \int_{\mathcal{W}} p(D_{tr}|\mathbf{w}')p(\mathbf{w}') d\mathbf{w}' \quad (13)$$

which is often ignored as a proportionality constant. We typically compute $p(\mathbf{w}|D_{tr})$ in log-form.

For a new point \mathbf{x}' , the predictive distribution over output Y' is:

$$p(Y'|\mathbf{x}', D_{tr}) = \int_{\mathcal{W}} p(Y'|\mathbf{x}', \mathbf{w})p(\mathbf{w}|D_{tr}) d\mathbf{w} \quad (14)$$

where $p(Y'|\mathbf{x}', \mathbf{w})$ is the same likelihood as in (12). $Y'|\mathbf{x}', D_{tr}$ is known as the **posterior predictive** (distribution). Point estimates of $p(Y'|\mathbf{x}', D_{tr})$, e.g. the posterior predictive mean, can be used if a concrete output prediction is desired. Since (14) is intractable, we typically sample a finite set of parameters and compute a Monte Carlo estimator.

Performing Bayesian inference (11) on deep neural networks $\Phi_{\mathbf{W}}$ (with weights and biases parametrized by \mathbf{W}) results in a **Bayesian neural network** (BNN).

A.1 Likelihoods for BNNs

The likelihood is purely a function of the model prediction $\Phi_{\mathbf{w}}(\mathbf{x})$ and the correct target y and does not depend on \mathbf{W} directly. As such, BNN likelihood distributions follow the standard choices used in other probabilistic models.

For regression, we model output noise as a zero-mean Gaussian: $\epsilon \sim \mathcal{N}(0, \sigma_{\epsilon}^2)$ where σ_{ϵ}^2 is the variance of the noise, treated as a hyperparameter. The likelihood PDF is then simply the Gaussian $Y \sim \mathcal{N}(\Phi_{\mathbf{w}}(\mathbf{x}), \sigma_{\epsilon}^2)$.

For K -classification, we specify the neural network to have K output nodes over which a softmax function is applied, hence the network outputs class probabilities². The likelihood PDF is then simply the value of the node representing class k : $\Phi_{\mathbf{w}}(\mathbf{x})_k$.

A.2 Priors for BNNs

For convenience and tractability, the common choice is an isotropic Gaussian $\mathbf{W} \sim \mathcal{N}(\mathbf{0}, \sigma_{\omega}^2 \mathbf{I})$, first proposed by MacKay [20], where σ_{ω}^2 is the shared variance for all individual weights. Neal [21] shows that in the regression setting, the isotropic Gaussian prior for a BNN with a single hidden layer approaches a Gaussian process prior as the number of hidden units tends to infinity, so long as the chosen activation function is bounded. We will use this prior in the baseline BNN for our experiments.

A.3 Posterior Inference on BNNs

As exact posterior inference via (11) is intractable, we instead rely on approximate inference algorithms, which can be broadly grouped into two classes based on their method of approximation.

¹For probability distributions, we abbreviate $p(\mathbf{W} = \mathbf{w})$ as $p(\mathbf{w})$.

²A concrete label can be obtained by choosing the class with highest output value.

Markov chain Monte Carlo (MCMC) MCMC algorithms rely on sampling from a Markov chain whose equilibrium distribution is the posterior. In the context of BNNs, our Markov chain is a sequence of random parameters $\mathbf{W}^{(1)}, \mathbf{W}^{(2)}, \dots$ defined over \mathcal{W} , which we construct by defining the transition kernel.

In this paper, we use **Hamiltonian Monte Carlo (HMC)**, an MCMC variant that employs Hamiltonian dynamics to generate proposals on top of a Metropolis-Hastings framework [5, 22]. HMC is often seen as the *gold standard* for approximate BNN inference, as (i) MCMC algorithms sample from the true posterior (which makes them more accurate than VI approximations, discussed below) and (ii) HMC is the canonical MCMC algorithm for BNN inference³. However, as HMC is inefficient and cannot scale with large or high-dimensional datasets, it is generally reserved for low-dimensional synthetic examples.

Variational Inference (VI) Variational learning for NNs [8, 10] approximates the true posterior $p(\mathbf{w}|D_{tr})$ with a variational distribution $q_{\theta}(\mathbf{w})$, which has the same support \mathcal{W} and is parametrized by $\theta \in \Theta$. The variational family $\mathbf{Q} = \{q_{\theta}|\theta \in \Theta\}$ is typically chosen to balance tractability and expressiveness. The Gaussian variational family is a common choice. To find the value of θ such that $q_{\theta}(\mathbf{w})$ is as similar as possible to $p(\mathbf{w}|D_{tr})$, we maximize a quantity known as the *Evidence Lower Bound* (ELBO):

$$\mathcal{L}_{\text{ELBO}}(\theta) = \mathbb{E}_{\mathbf{w} \sim q_{\theta}} \left[\log p(D_{tr}|\mathbf{W}) \right] - D_{KL}(q_{\theta}(\mathbf{w}) || p(\mathbf{w})) \quad (15)$$

Estimators for the integral in (15) are necessary. Once a tractable proxy is formulated, standard optimization algorithms can be used.

In this paper, we use **Bayes by Backprop (BBB)**, a VI algorithm that makes use of the so-called *reparametrization trick* [15] to compute a Monte Carlo estimator of (15) on a Gaussian variational family [4]. BBB is scalable and fast, and therefore can be applied to high-dimensional and large datasets in real-life applications.

We also use **Stein Variational Gradient Descent (SVGD)**, a VI algorithm that relies on applying successive transforms to an initial set of particles, in a way that incrementally minimizes the KL divergence between the empirical distribution of the transformed particles and $p(\mathbf{w}|D_{tr})$ [17]. SVGD is also scalable to high-dimensional, large datasets. Furthermore, the transforms that SVGD apply implicitly define a richer variational family than Gaussian approximations.

A.4 Prediction using BNNs

For all algorithms, prediction can be carried out by computing the Monte Carlo estimator of (14):

$$p(Y'|\mathbf{x}, D_{tr}) \approx \frac{1}{S} \sum_{i=1}^S p(Y'|\mathbf{x}', \mathbf{w}^{(i)}) \quad (16)$$

from S samples of the (approximate) posterior. We can construct credible intervals for any given \mathbf{x}' using the empirical quantiles of $\{\mathbf{w}^{(1)}, \dots, \mathbf{w}^{(S)}\}$, which allows us to quantify how confident the BNN is at \mathbf{x}' .

³MCMC methods “simpler” than HMC, such as naive Metropolis-Hastings or Gibbs sampling, are intractable on high-dimensional parametric models such as BNNs. As such, HMC is, in some ways, the simplest algorithm used for approximate BNN inference.

B Approximations for BNN Prior Predictive

We state the approximate forms for a variational BNN prior predictive $p_{\lambda}(\Phi_{\mathbf{W}}|\mathbf{x})$ in the case of regression and binary classification, where we assume a Gaussian variational family. Readers are referred to Chapter 5.7 of Bishop [3] for their derivations. We denote $\lambda = (\boldsymbol{\mu}, \boldsymbol{\sigma})$ as the variational parameters for the mean and standard deviation of each \mathbf{w}_i .

Approximation Prior Predictive for Regression A Gaussian approximation of the prior predictive is:

$$\Phi_{\mathbf{W}}|\mathbf{x} \sim \mathcal{N}(\Phi_{\boldsymbol{\mu}}(\mathbf{x}), \sigma_{\epsilon}^2 + \mathbf{g}^{\top}(\boldsymbol{\sigma}^2 \cdot \mathbf{g})) \quad (17)$$

where

$$\mathbf{g} = \left[\nabla_{\mathbf{w}} \Phi_{\mathbf{w}}(\mathbf{x}) \Big|_{\mathbf{w}=\boldsymbol{\mu}} \right] \quad (18)$$

As noted in Appendix A, σ_{ϵ} is the standard deviation of the output noise that we model.

Approximation Prior Predictive for Binary Classification We will need to make a slight modification to the BNN setup. Typically, a BNN for K -classification has K output nodes, over which a softmax function is applied such that the output values sum to 1 (representing predicted class probabilities). Here, instead of using a BNN with 2 output nodes, we will use a BNN with a single output node, over which we apply the logistic sigmoid function ⁴:

$$\sigma_L(x) = \frac{e^x}{e^x + 1} \quad (19)$$

The resulting value is then interpreted as the probability that the predicted output is 1 (the ‘‘positive’’ class):

$$\Phi_{\mathbf{w}}(\mathbf{x}) = p(Y = 1|\mathbf{x}) = \sigma_L(\phi_{\mathbf{w}}(\mathbf{x})) \quad (20)$$

where $\phi_{\mathbf{w}}(\mathbf{x})$ represents the output node’s value *before* applying the sigmoid function. Note that $p(Y = 0|\mathbf{x}) = 1 - p(Y = 1|\mathbf{x})$. With this, the approximation for the prior predictive is given as:

$$p_{\lambda}(\Phi_{\mathbf{W}}(\mathbf{x}) = 1|\mathbf{x}) = \sigma_L \left(\left(1 + \frac{\pi(\mathbf{g}^{\top}(\boldsymbol{\sigma}^2 \cdot \mathbf{g}))}{8} \right)^{-1/2} \mathbf{g}^{\top} \boldsymbol{\mu} \right) \quad (21)$$

where

$$\mathbf{g} = \left[\nabla_{\mathbf{w}} \phi_{\mathbf{w}}(\mathbf{x}) \Big|_{\mathbf{w}=\boldsymbol{\mu}} \right] \quad (22)$$

Note that the first-order derivative \mathbf{g} here is taken w.r.t. $\phi(\mathbf{x})$, not $\Phi(\mathbf{x})$.

⁴The logistic sigmoid function derives its name from logistic regression, a simpler statistical model used for classification. The softmax function can be seen as a generalization of the logistic sigmoid function for $K > 2$.

C Experimental Details

All the details listed below can also be found at: <https://github.com/dtak/ocbnn-public>.

C.1 Low-Dimensional Simulations

The model for all experiments is a BNN with a single 10-node RBF hidden layer. The baseline BNN uses an isotropic Gaussian prior with $\sigma_\omega = 1$. The output noise for regression experiments is modeled as $\sigma_\epsilon = 0.1$.

We run HMC for inference unless noted otherwise. When HMC is used, we discard 10000 samples as burn-in, before collecting 1000 samples at intervals of 10 (a total of 20000 Metropolis-Hastings iterations). $L = 50$, and ϵ is variably adjusted such that the overall acceptance rate is ~ 0.9 . When SVGD is used, we run 1000 update iterations of 50 particles using AdaGrad [6] with an initial learning rate of 0.75. When BBB is used, we run 10000 epochs using AdaGrad with an initial learning rate of 0.1. $\theta = (\mu, \sigma)$ is initialized to 0 for all means and 1 for all variances. Each epoch, we draw 5 samples of ϵ and average the 5 resulting gradients. 1000 samples are collected for prediction.

In Figure 1, the hyperparameters for the negative exponential COCP are: $\gamma = 10000$, $\tau_0 = 15$ and $\tau_1 = 2$. In Figure 2, the hyperparameters for the positive Dirichlet COCP are: $\alpha_i = 10$ if $i \in \mathcal{C}_y(\mathbf{x})$, and 1.5 otherwise. In Figure 3a and Figure 4, we run 125 and 50 epochs of AOCOP optimization respectively. $\lambda = (\mu, \sigma)$ is initialized to 0 for all means and 1 for all variances. The AdaGrad optimizer with an initial learning rate of 0.1 is used for optimization. In Figure 3b, the hyperparameters for the negative exponential COCP are: $\gamma = 10000$, $\tau_0 = 15$ and $\tau_1 = 2$. In Figure 6, the positive Gaussian COCP is used for all 3 constraints with $\sigma_C = 1.25$. The training data is perturbed with Gaussian noise with mean 0 and standard deviation 1.

C.2 High-Dimensional Applications

Clinical Action Prediction The MIMIC-III database [12] is a freely accessible benchmark database for healthcare research, developed by the MIT Lab for Computational Physiology. It consists of de-identified health data associated with 53,423 distinct admissions to critical care units at the Beth Israel Deaconess Medical Center in Boston, Massachusetts, between 2001 and 2012. From the original MIMIC-III dataset, we performed mild data cleaning and selected useful features after consulting medical opinion. The final dataset contains 8 features and a binary target, listed below. Each data point represents an hourly timestamp, however, as this is treated as a time-independent prediction problem, the timestamps themselves are not used as features.

- **MAP:** Continuous. Mean arterial pressure. Standardized.
- **age:** Continuous. Age of patient. Standardized.
- **urine:** Continuous. Urine output. Log-transformed.
- **weight:** Continuous. Weight of patient. Standardized.
- **creatinine:** Continuous. Level of creatinine in the blood. Log-transformed.
- **lactate:** Continuous. Level of lactate in the blood. Log-transformed.
- **bicarbonate:** Continuous. Level of bicarbonate in the blood. Standardized.
- **BUN:** Continuous. Level of urea nitrogen in the blood. Log-transformed.
- **action (target):** Binary. 1 if the amount of either vasopressor or IV fluid given to the patient (at that particular time step) is more than 0, and 0 otherwise.

The model for all experiments is a BNN with two 150-node RBF hidden layers. For the baseline prior, $\sigma_\omega = 1$. BBB is used for inference with 20000 epochs. $\theta = (\mu, \sigma)$ is initialized to 0 for all means and 1 for all variances. The AdaGrad optimizer with an initial learning rate of 1.0 is used. As the dataset is imbalanced, the minority class ($\text{action} = 1$) is evenly upsampled. Points in \mathcal{C}_x were intentionally filtered from the training set. The training set is also batched during inference for efficiency. The positive Dirichlet COCP is used with $\alpha_0 = 2$ and $\alpha_1 = 40$.

Recidivism Prediction The team behind the 2016 ProPublica study on COMPAS created a dataset containing information about 6172 defendants from Broward County, Florida. We followed the same data processing steps as [16]. The only additional step taken was standardization of all continuous features. The final dataset contains 9 features and a binary target:

- `age`: Continuous. Age of defendant.
- `two_year_recid`: Binary. 1 if the defendant recidivated within two years of the current charge.
- `priors_count`: Continuous. Number of prior charges the defendant had.
- `length_of_stay`: Continuous. The number of days the defendant stayed in jail for the current charge.
- `c_charge_degree_F`: Binary. 1 if the current charge is a felony.
- `c_charge_degree_M`: Binary. 1 if the current charge is a misdemeanor.
- `sex_Female`: Binary. 1 if the defendant is female.
- `sex_Male`: Binary. 1 if the defendant is male.
- `race`: Binary. 1 if the defendant is African American.
- `compas_high_risk (target)`: Binary. 1 if COMPAS predicted the defendant as having a high risk of recidivism, and 0 otherwise.

The model for all experiments is a BNN with two 100-node RBF hidden layers. For the baseline prior, $\sigma_\omega = 1$. SVGD is performed with 50 particles and 1000 iterations, using AdaGrad with an initial learning rate of 0.5. The dataset is batched during inference for efficiency. The AOCP is used with $\lambda = (\mu, \sigma)$ initialized to 0 for all means and 1 for all variances. 50 epochs of optimization are performed using AdaGrad at an initial learning rate of 0.1. We draw 30 samples from the convex hull of D_{tr} each iteration to compute the approximation for (9). The optimized variance parameters are shrunk by a factor of 30 to 40 for posterior inference.

Credit Scoring Prediction The Give Me Some Credit dataset ($N = 133K$) [13], taken from a 2011 Kaggle competition, contains 10 features and a binary target:

- `RevolvingUtilizationOfUnsecuredLines`: Continuous. Total balance on credit cards and personal lines of credit (except real estate and no installment debt like car loans), divided by the sum of credit limits.
- `age`: Discrete. Age of borrower in years. Standardized.
- `DebtRatio`: Continuous. Monthly debt payments, alimony, and living costs, divided by monthly gross income.
- `MonthlyIncome`: Continuous. Monthly income. Standardized.
- `NumberOfOpenCreditLinesAndLoans`: Discrete. Number of open loans and lines of credit. Standardized.
- `NumberRealEstateLoansOrLines`: Discrete. Number of mortgage and real estate loans, including home equity lines of credit.
- `NumberOfTime30-59DaysPastDueNotWorse`: Discrete. Number of times borrower has been 30 to 59 days past due (but no worse) in the last 2 years.
- `NumberOfTime60-89DaysPastDueNotWorse`: Discrete. Number of times borrower has been 60 to 89 days past due (but no worse) in the last 2 years.
- `NumberOfTimes90DaysLate`: Discrete. Number of times borrower has been 90 days or more past due in the last 2 years.
- `NumberOfDependents`: Discrete. Number of dependents in family, excluding themselves.
- `SeriousDlqin2yrs (target)`: Binary. 1 if the individual experiences serious financial distress within two years.

The model for all experiments is a BNN with two 50-node RBF hidden layers. For the baseline prior, $\sigma_\omega = 1$. BBB is used for inference with 10000 epochs. $\theta = (\mu, \sigma)$ is initialized to 0 for all means and e for all variances. The AdaGrad optimizer with an initial learning rate of 0.1 is used. As the dataset is imbalanced, the minority class (`action = 1`) is evenly upsampled. The dataset is batched during inference for efficiency. The positive Dirichlet COCP is used with $\alpha_0 = 10$ and $\alpha_1 = 0.05$.

D Additional Results

Below, we show additional plots referenced in Section 5.

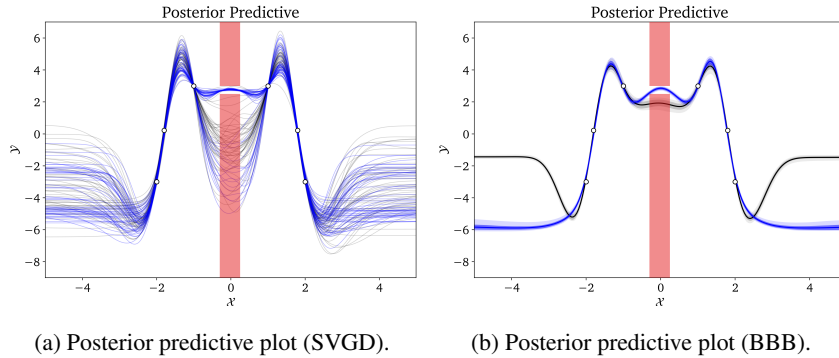


Figure 5: Same experimental setup as in Figure 1, except that (a) uses SVGD and (b) uses BBB for posterior inference. Like HMC, both posterior predictive plots obey the constraints and fit D_{tr} . As in Figure 3b, SVGD produces an OC-BNN posterior that still violates the constraint to a small degree, as SVGD particles are optimized to be as far from each other (in \mathcal{W}) as possible. BBB produces a posterior that has smaller variance than HMC or SVGD everywhere in \mathcal{X} . Underestimation of variance is a commonly observed problem with VI methods.

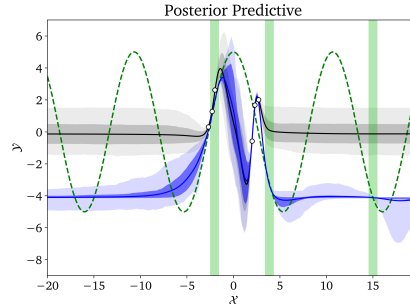


Figure 6: The ground-truth function (dotted green curve) is $y^* = 5 \cos(x/1.7)$. D_{tr} contains 6 points perturbed by large Gaussian noise around ground-truth values. Three positive constraints (vertical green bands on \mathcal{C}_x) are also placed using positive Gaussian COCPs around the corresponding ground-truth values. The resulting OC-BNN posterior predictive “overfits” to both the noisy data and all three constraints.